ELSEVIER

Applied Surface Science 192 (2002) 258–269

applied surface science

www.elsevier.com/locate/apsusc

Modeling of magnetron sputtering plasmas

C.H. Shon, J.K. Lee*

Department of Electrical Engineering, Pohang University of Science of Technology, Pohang 790-784, South Korea

Abstract

Partially ionized, low-temperature plasmas have been used extensively in many areas of technology. These applications of plasma include surface processing and lighting devices. There are three major categories in surface processing: sputtering, etching and surface modification. The examples of lighting device application are light bulbs, lasers and plasma display devices. In this discussion, simulation study of magnetron sputtering system are reviewed and future issues of these systems are discussed. A two-dimensional three-velocity particle-in-cell (PIC) code is used to simulate kinetic plasma properties in a planar magnetron system with realistic magnetic fields in two and three dimensions. Various plasma characteristics and erosion profiles of a target material are obtained with these magnetic fields. Scaling formulas are used in order to estimate the steady-state properties of plasma and reduce computation time. Variations in the geometry and the magnetic field optimize these erosion profiles and plasma characteristics. For the plasma characteristics, we also calculate the plasma temperature and the velocity distribution function. The velocity distribution function of electrons is nearly Maxwellian, while that of ions is non-Maxwellian. The electron temperature in the bulk coincides well with the experimentally measured values. The majority of ions are in the energy range below half of the applied voltage. © 2002 Published by Elsevier Science B.V.

PACS: 52.25.Xz; 52.65.Pp; 52.65.Rr; 52.80.Hc

Keywords: Low-temperature plasma; Magnetron sputter; Kinetic simulation; Particle-in-cell; Monte Carlo

1. Introduction

There has been an enormous growth in the use of partially ionized, low-temperature plasmas in many areas of technology during last 30 years or so. Surface processing is one example of these technology. Surface processing consists of deposition, etching and implantation (surface modification). In this discussion, we focus on the simulation study of DC magnetron sputtering system. As microelectronics industry grows exponentially, fabrication of thin film process becomes crucial point of concern. Deposition process that uses magnetron discharge is widely used in the microelectronics industry. Magnetron sputtering [1–6] is the major method that has been used for coating thin films. It is also used for coating large-area display panels and inner wall of ceramics tubes [7]. Many research activities about magnetron sputter have been carried out by experimental methods and by modeling. Modeling by numerical simulation and theory generate realistic and useful results that can be compared with experiment.

Taking advantage of the magnetic field, magnetron sputter operates at low pressure and low voltage conditions. The applied magnetic field confines energetic electrons near the cathode. These confined electrons ionize neutral gas and form a high-density plasma near the cathode surface. The ions produced

* Corresponding author. Tel.: +82-54-279-2083; fax: +82-54-279-2903.
E-mail address: jkl@postech.ac.kr (J.K. Lee).

0169-4332/02/$ – see front matter
PII: S0169-4332(02)00030-2

by these electrons are accelerated towards the cathode surface with high energy. The bombardment of ions not only sputter out the target material but also produces secondary electrons that maintain the discharge. The research fields about modeling of magnetron sputtering are plasma characteristics, effects of applied magnetic field, background neutral gas transport, erosion of target materials and deposition of sputtered atoms, etc.

There are many simulation results about the plasma characteristics [8–14] in magnetron sputter. Usually particle-in-cell/Monte Carlo collision (PIC/MCC) technique has been used for the modeling of magnetron sputter. Recently, hybrid model that combines particle and fluid model has been developed [15] to reduce computation time. There is another kinetic approach that solves Boltzmann equation [16], which provides distribution functions and swarm parameters for fluid modeling with arbitrarily electric and magnetic field orientations.

Together with the plasma characteristics, erosion profile of target material is an important concern in magnetron sputtering because of target utilization. Usually Monte Carlo (MC) method has been used to obtain erosion profiles [17–20] and reduce the experimental efforts. This technique has also been used for the deposition of atoms from cathode surface onto the substrate. There are attempts to simulate transport and deposition of sputtered atoms self-consistently by MC method [17,21–26]. As the discharge occurs, transport and temperature distribution of background neutral gas become important because background gas heating and associated local density variations can affect both the physical processes in the plasma and the properties of the growing films [27,28]. PIC plus direct simulation Monte Carlo (PIC–DSMC) approach is proposed to simulate the plasma, neutral gas and surface reactions (sputtering and deposition) self-consistently [29].

In Section 2, the geometry of magnetron sputter and two-dimensional (2D) and three-dimensional (3D) simulation results are presented. In Section 3, the results of MC simulation is presented for erosion profiles, sputtered atoms transport and background neutral gas transport. The distribution functions of electrons and ions within magnetron sputter is discussed in Section 4. Section 5 summarizes our works.

2. Geometry and magnetic fields

2.1. Simulation geometry

There are many devices for plasma processing. However it is nearly impossible to choose the best plasma device for all applications because of the complex parameter space associated with the equipment. Until now, the most common plasma for the processing is low pressure glow discharge. The pressure range is from 10^{-4} to 10 Torr and the electron density is usually from 10^9 to 10^{12} cm^{-3}. The pressure is determined by the particular application. In the sputter deposition, low pressure is preferred in order to make the ions move towards the target material without collisions in the sheath region, which preserves the ion kinetic energy. Another advantage of low pressure is less collisions between sputtered atoms and neutral gas, which reduces the scattering of sputtered atoms to the walls of the system or back to the target surface.

Fig. 1 shows a typical 2D magnetron geometry with cathode, substrate, anode and magnets. Usually, the cathode is negatively biased with 400–600 V with other conductors grounded. The magnets located below the cathode plate are assembled to form either a racetrack-type geometry or a circular one in the third dimension. Pole pieces are usually equipped with the magnets to concentrate the magnetic field. Cooling water flows under the cathode plate. The substrate is grounded or floated. There are many other geometries

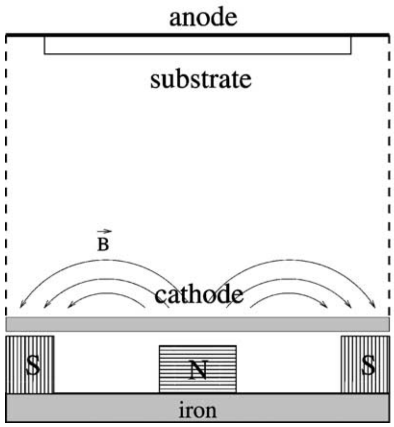

Fig. 1. Schematic diagram of typical magnetron sputtering system.

for the magnetron sputter, but a more detailed discussion is found elsewhere [30].

Magnetic fields that come from various magnet geometries can be used to optimize the geometry of magnetron sputter. The effects of magnetic field are lowering the breakdown voltage and making high-density plasma in the system. Magnetic field makes it possible to operate sputtering system in lower pressure than the one necessary to initiate discharge for a fixed applied voltage from the Paschen theory. The applied magnetic field traps electrons to increase their number density, which increases the ion density by ionizing the neutral gas. This leads to higher ion bombardment and higher sputtering rates at the cathode target. Therefore the changes of voltage, pressure and magnetic field affect not only plasma characteristics but also the deposited thin film properties.

2.2. Plasma characteristics

The plasma characteristics and target erosion profiles are closely related to the geometry and magnetic field profiles of a system. As the magnetic field is not simple, an analytical solution of plasma motion is not usually obtained. Some efforts have been made to analyze the plasma characteristics in one-dimensional geometry under a constant magnetic field [31,32]. The plasma characteristics are obtained by semi-analytic

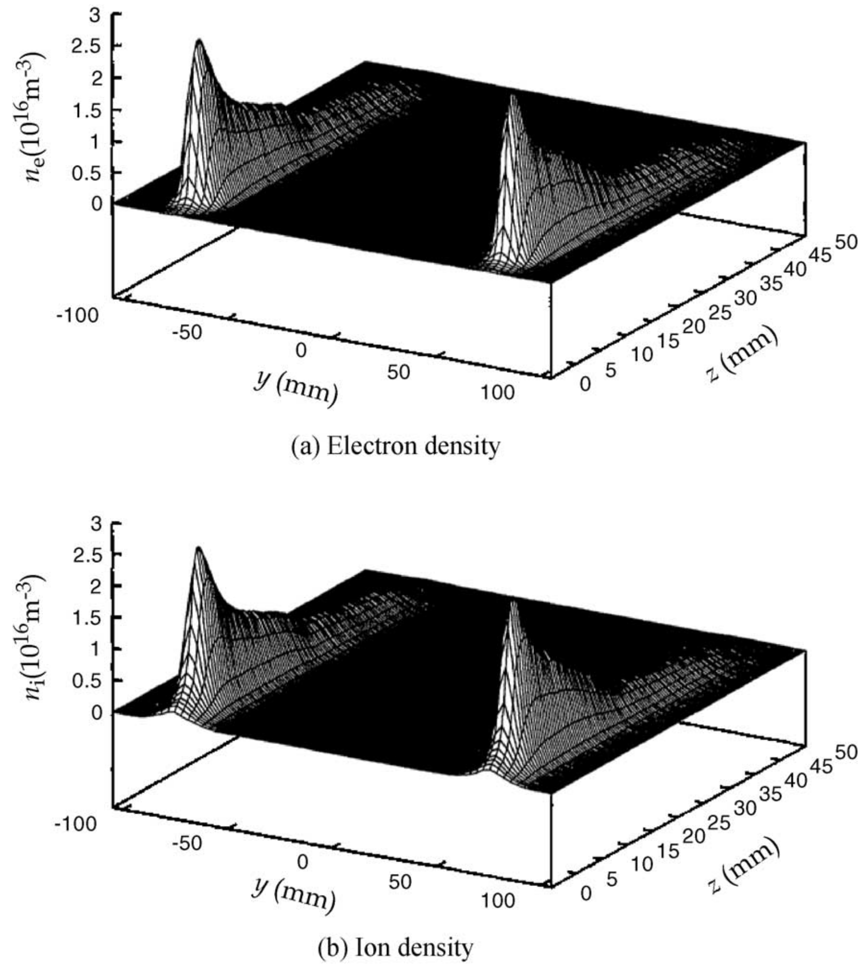

Fig. 2. Number densities of electrons and ions in the *yz*-plane. *z*-direction is from cathode to substrate (from [8]).

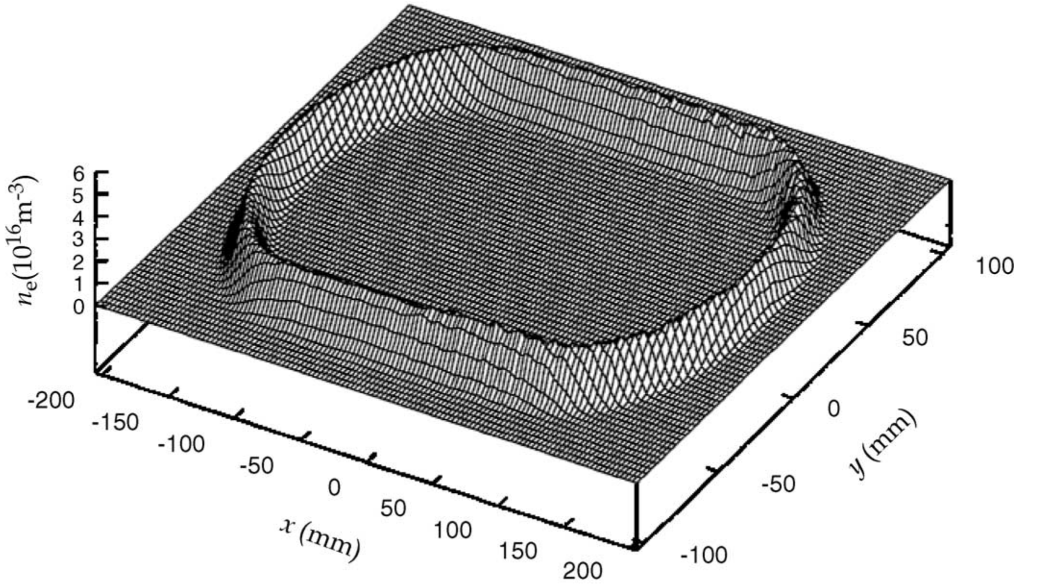

Fig. 3. Number densities of electrons in the xy-plane. z-direction is from cathode to substrate (from [8]).

fluid method. There are also experimental measurements for the radial and axial distributions of plasma in cylindrical magnetron sputter, which are compared with theory [2,4]. In general, the space-charge limited current in a plane diode is given by the Child–Langmuir law [33]:

$$\bar{J}_d = \frac{4\epsilon_0}{9}\sqrt{\frac{2e}{M}}\frac{V_c^{3/2}}{s^2}, \quad (1)$$

where ϵ_0 is permittivity, e the particle charge, M the mass, V_c the sheath voltage and s the sheath size. Gu and Lieberman [2,5] proposed a new scaling:

$$s_{GL} = C\frac{V^{7/8}}{I^{1/2}B^{1/4}}, \quad (2)$$

and compared this with their optical emission measurement, where C is the proportionality constant, V the applied voltage, I the discharge current and B the magnetic field strength. Although the experimental sheath size is almost twice higher than the value calculated from Eq. (2), the scaling of experimental sheath size with magnetic field (B) agrees well with Child–Langmuir equation (1). There is a proposal to substitute the sheath length with Larmor radius of electrons which have average kinetic energy, eV_a, as a result of investigations in an optical emission experiment [3].

There are many simulations for the plasma characteristics in the sputtering system. Nanbu and Kondo [8] has been doing 3D simulations of plasma in racetrack-type planar magnetron system. The PIC/MC method is used to simulate the system. The plasma profiles of magnetron sputtering system are shown in Figs. 2 and 3. Fig. 2 shows the plasma profiles of yz plane, where z-direction is from cathode to anode. Fig. 3 shows the electron density at $z = 9.8$ mm above the cathode plate, where the electron density is maximum. The sheath thickness of the simulation is compared with Eq. (2), which showed good agreement. The sheath thickness decreases with increasing magnetic field, but does not have relationship with gas pressure. The electric field and plasma density increase with magnetic field. The distribution of ion flux on to the cathode is strongly correlated to the peak plasma density.

There is another PIC/MC 2D simulation of sputtering system [14,34]. The 2D simulation results are similar with the 3D results of Nanbu's, but the steady-state properties are determined by the Child–Langmuir law in which the sheath thickness is substituted with Larmor radius. The electric field in the sheath region shows a linear dependence in the simulations, which means that the ion distribution is uniform in this region in order to make a matrix sheath. Laser induced fluorescence (LIF) experiment shows similar results [6]. The PIC/MC method calculates the plasma profiles and potential (electric field) self-consistently, allowing plasma distribution and potential affect each other. There are other methods that assume a pre-defined potential and simulate particles with the potential [9,18]. The electric potential sheath region is modeled by Child–Langmuir law. The ionization profile is compared with the experimental one and used to obtain the erosion profile.

As an improvement for the PIC/MC model that requires a large computation time, hybrid model has been developed [15]. In this model, high energy electrons or total electrons are traced by MC technique to estimate the non-local ionization rate, bulk electrons and ions are treated by fluid model in order to reduce computation time. Kinetic approach that solves Boltzmann equation has also been developed and used for the estimation of plasma distribution function of electrons and ions in a given electric and magnetic field [16].

3. Erosion and deposition of atoms

3.1. Simulation of target erosion

Erosion of a target mainly occurs by energetic ions in plasmas and if due to sputtering is formed inhomogeneously because the distribution of plasmas occurs inhomogeneously as in Fig. 2. The nonuniformity of plasma originates from the magnetic fields that magnetize and confine electrons in small regions. The inhomogeneity of erosion makes the lifetime of a target short and usage of the target less effective. In particular for a ferromagnetic target, the configuration of magnetic fields is modified considerably with the progress of erosion and results in the localization of plasmas in the eroded area, whereby erosion becomes even more localized. In order to fabricate thin film efficiently and utilize target homogeneously, it is important to analyze the process of erosion formation.

As the erosion profile is strongly correlated to the flux of ions towards the target surface, ion distribution is important to estimate the erosion profile. There are several methods to calculate the erosion profiles. First, the erosion profile is obtained by the distribution of ions, which is determined by the ionization points [9,18]. As the pressure is low enough, the collisions between ions and neutral gas are ignored. The ions are assumed to be unaffected by the applied magnetic field because the Larmor radius of ion exceeds the system size under usual magnetic field strength (several hundreds Gauss) in sputtering system, and therefore their trajectories are straight towards the target. This method is very simple and fast because only electrons are followed by MC method in a pre-defined potential. The disadvantage of this method is that the energy and angle distribution of ions cannot be obtained. The energy and angle of incident ions onto the target are important to obtain the exact sputtering rate of the target.

Second, ion trajectories are followed with electrons by MC method in a pre-defined potential [11]. The energy, angle and spatial distributions are obtained in the model and used to determine the probability of sputtering and other ion–surface interactions. Fig. 4 shows the comparisons between simulation and experiment. The ion impact densities are calculated with three conditions: (1) no collisions and no turbulent electric field; (2) collisions but no turbulent electric field; (3) both collisions and a turbulent electric field. A turbulent electric field included in the ion simulation is based on Langmuir probe measurements [35]. They reported that the fluctuations are probably ion-acoustic waves that grew from a current-driven instability in the plasma. Fig. 4 shows the

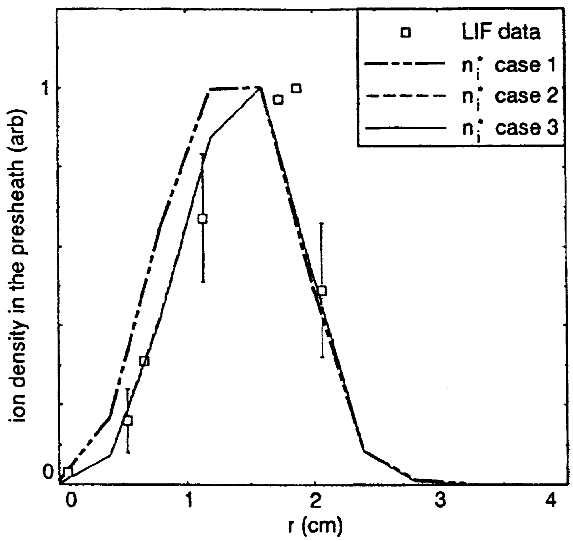

Fig. 4. The comparison of radial density profiles between experiment and simulations for three different conditions (from [11]).

comparison of density profiles between experiment and simulations for three cases mentioned above. Cases 2 and 3 include collisions with neutrals and show the best agreement. Including turbulence in the simulation (case 3) has little effect.

Thirdly, ion flux from the PIC/MC simulation is used for the estimation of erosion profiles of target material [14]. In this method, the plasma transport and space potential are calculated self-consistently, where assumption for space potential is not needed. In PIC/MC code, not only collisions between plasma and neutral gas but also the energy and angle distributions of ions are followed. The ion flux, energy and angle distribution onto the target surface is obtained from the simulation. Fig. 5 shows a comparison of the simulation and the experiment. The experimental erosion width is larger than that of simulation, but in experiment the erosion occurs during long time scale. Therefore the time development of erosion of target surface must be included in the simulation to be compared with experiment. The pre-eroded target geometry is used to include the effect of geometrical variation of target surface with time [14]. As shown in the figure, the erosion profiles become broad with time.

Above methods concentrate on the effects of plasma distributions which make erosion profiles. There is another MC model that focuses on the topographical variation considering surface reactions: sputtering, ion reflection, redeposition and surface diffusion [36]. But this kind of calculation needs the exact information about the ion flux, energy and angle distributions towards the surface. The combination of this and PIC/MC method will be very useful to obtain the self-consistent profiles of target erosion. Besides, more data for chemical and physical reactions on the surface are required for more accurate results. The evolution of erosion profiles have also been obtained and compared with experiments [37] by simulating the ion and fast neutral transport in the sheath region with Boltzmann equation and the database of the 2D hybrid model [15].

3.2. Transport and deposition of sputtered atoms

Much effort has been made to trace the sputtered atoms from target surface to substrate, which is useful to estimate thin film profiles on the substrate [17,21–26]. The transport of sputtered atoms are affected mainly by the elastic collisions with the background gases. The thermalization of various sputtered atoms and reflected neutrals are simulated in Ref. [21]. The energies of sputtered atoms are calculated with various values of (pressure) $\times$ (distance between target and substrate) for various kinds of sputtered atoms and background neutrals. Motohiro [22] compared the simulation results with experiment. The effect of the mass and binding energy for sputtered atoms, and the pressure of the background filling gas (Ar only) on the sputtered atoms

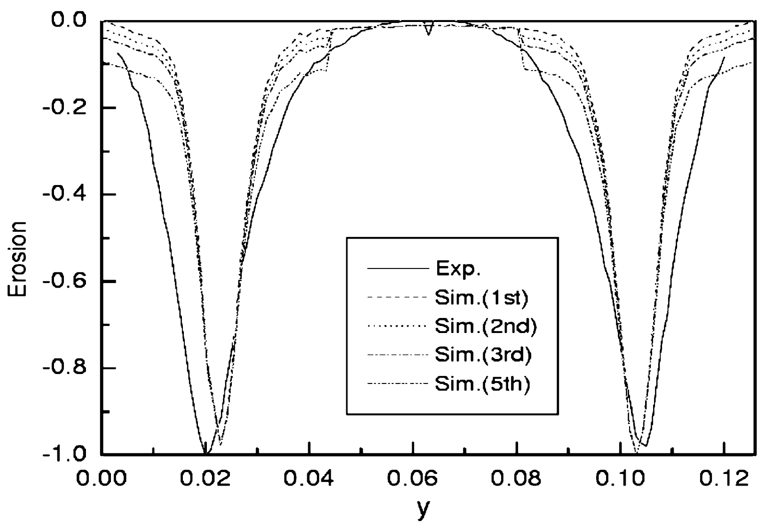

Fig. 5. Comparison of erosion between simulation and experiment.

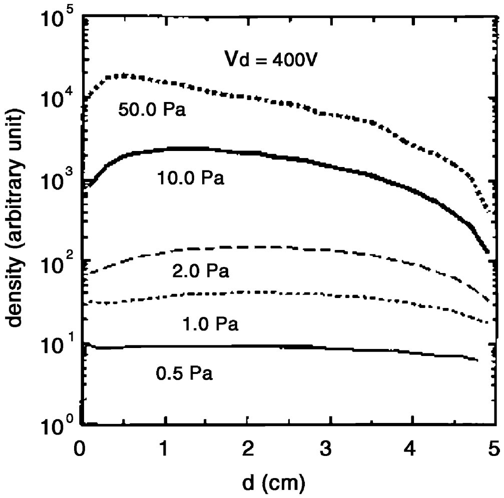

Fig. 6. The density profiles of sputtered atoms at various pressures (from [25]). d is cathode–substrate separation and discharge voltage is 400 V.

arriving at a substrate surface are simulated by Turner et al. [23]. The spatial profiles of density, energy and angle of incidence on substrate are also calculated. The atomic collisions in the cathode, which leads to sputtering and reflection, and thermalization of sputtered atoms are simulated by Yamamura and Ishida [25]. One of the results is shown in Fig. 6, which shows the density profiles of sputtered Cu atoms at various pressures.

In the magnetron system, high current flows, correspondingly large fluxes of target atoms are sputtered out from the cathode. These atoms deliver energy and momentum to the background neutral gas. As a result, the neutral gas in front of cathode heats up and flows outward from the sheath region (sputtering wind) [38], which results in the rarefaction of the neutral gas [39]. Therefore the collisions between neutrals and sputtered atoms are reduced in front of the cathode in a high current discharge. The coupled system of sputtered atoms and neutral gas using DSMC algorithm has been used to calculate the distribution of sputtered atoms [24]. Fig. 7 shows the steady-state behavior of sputtered Cu atoms in a DSMC simulation. The simulation is self-consistent in that the reaction of the sputtered atoms on the discharge gas and back-reaction is fully taken into account. A strong temperature increase occurs in front of the cathode, which is a

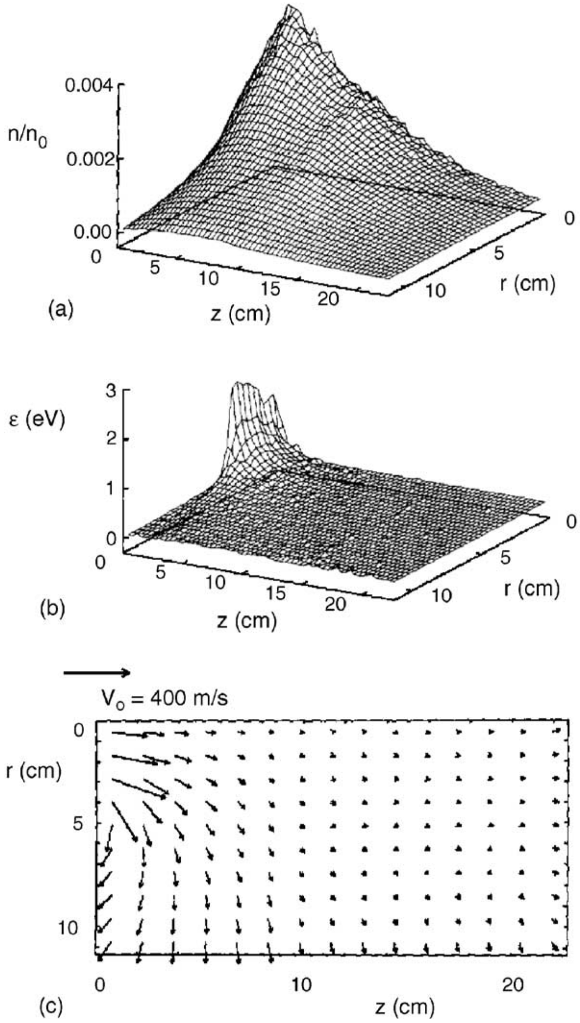

Fig. 7. Steady-state behavior of sputtered Cu atoms in a DSMC simulation: (a) density n; (b) mean kinetic energy per particle, ϵ; (c) velocity fluid u (from [24]).

result of the transfer of energy from sputtered atoms to background gas.

The deposition rate of the sputtered atoms is compared with the experiment including the reemission of sputtered atoms deposited onto the target surface and angle dependency of incident ions in Ref. [17]. The deposition profile that depends on the magnetic field shape and the geometry of magnetron sputter is calculated with an assumption that the sputtered atoms from the target surface are scattered isotropically to reach the substrate without engaging collisions with

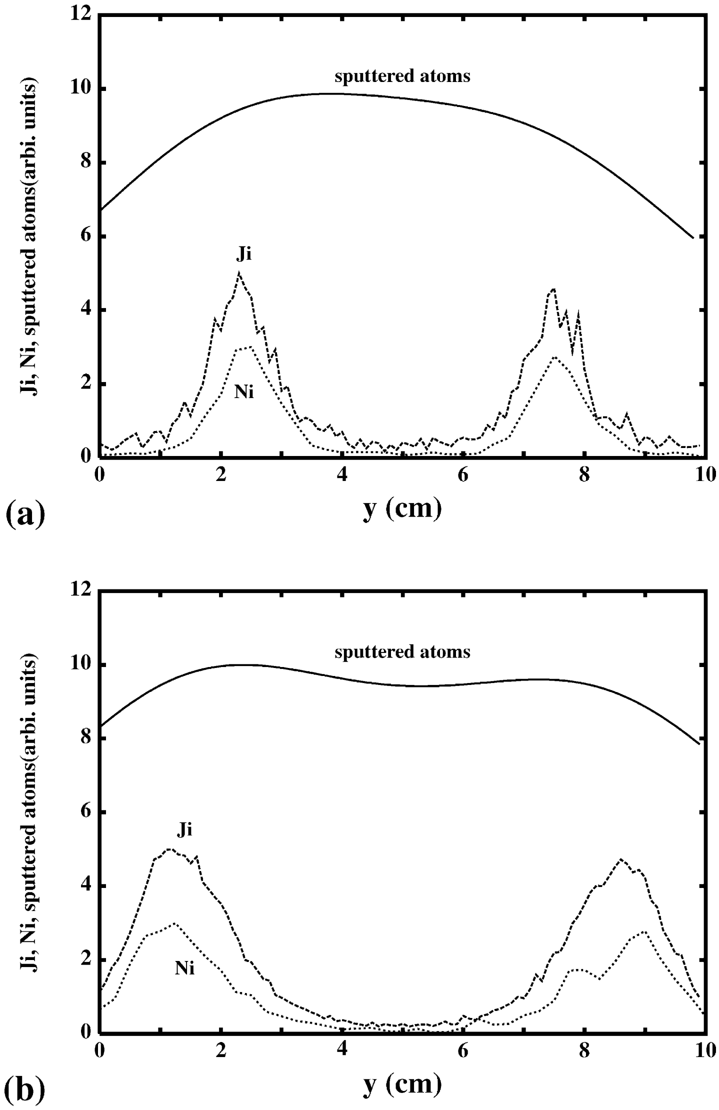

Fig. 8. Deposition profiles dependent on different magnetic field distributions (from [34]).

neutral gas [34]. As the peak points are shifted towards the edges, the deposited atom density at the substrate is flattened for an optimized deposition profile (Fig. 8). The impact angle and energy distributions of multi-component sputtered atoms onto the substrate have been simulated by Nathan et al. [26].

3.3. Neutral gas transport

As stated in the Section 3.2, the neutral gas density and temperature distributions are important to simulate the sputtered atom transport. Moreover they are related to the plasma distribution and energetic neutral gas sputtering. The plasma density distributions are highly correlated to the neutral gas density and temperature distribution through collision processes. Therefore the transport of sputtered atoms and background neutral gas are correlated to each other and are not separated. The neutral gas heating and rarefaction are closely related to the target material and background gas species because of different energy transfer and different thermal conductivity of the neutral gas. The neutral gas transport models [27–29] have been included in the calculation of sputtered atom transport models.

Turner [27] has simulated the neutral gas rarefaction and temperature distributions with various kinds of sputtered atoms that have different binding energies. The neutral gas temperature distributions are also calculated, where power input is included in the heat transfer model [28]. Fig. 9 shows the temperature distributions of background neutral gas. As the neutral gas distributions not only change the trajectories of sputtered atoms but also the plasma profiles in the system, the unified simulation of plasma, background neutral gas and sputtered atoms. In this kind of simulation [29], the plasma, background neutrals and sputtered atoms are simulated self-consistently with little assumptions.

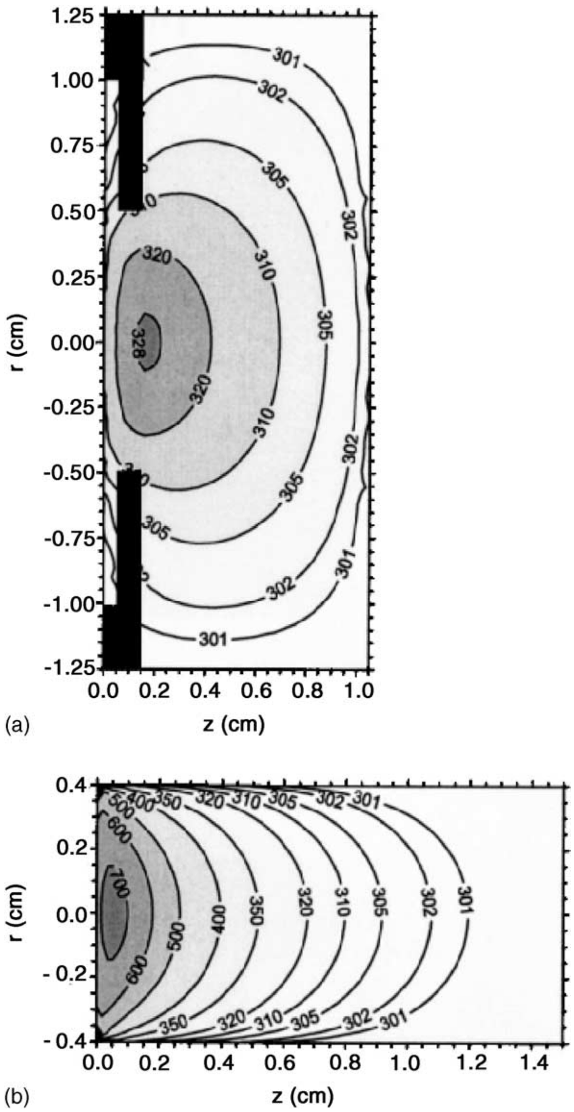

Fig. 9. 2D background gas temperature profile. The cathode is found at the left end of both figures, whereas the other boundaries represent the anodes (from [28]).

4. Distribution functions in magnetron sputter

Electron and ion energy distributions are important and useful for many practical purposes. The velocity distribution functions of electrons and ions at the cathode are obtained from MC or PIC/MC simulations. Energy and temperature distributions are obtained from the velocity distributions of particles. There have been attempts to figure out the distributions of plasma with simulation and experiment by Goree and coworkers [11,40]. There is another approach that solves the Boltzmann equation to obtain electron energy distribution function (EEDF) and plasma profiles [41].

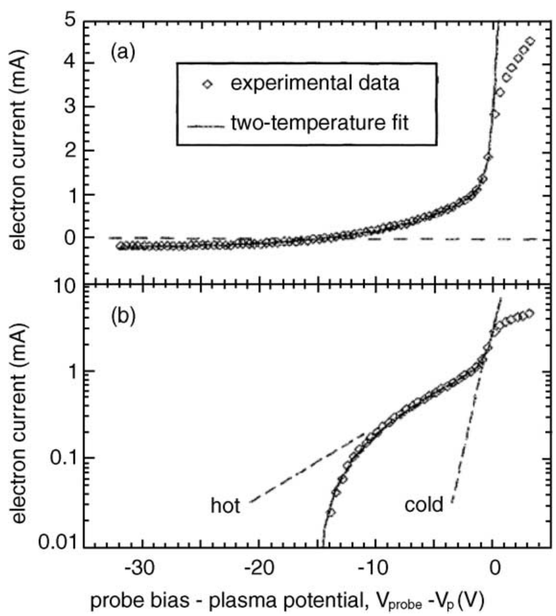

Fig. 10. Two-temperature probe characteristics in: (a) the electron current with two-temperature fitting; (b) log scale of electron current that shows two slopes (from [40]).

Fig. 10 shows an experimental result of two-temperature electron distribution. Two slopes in Fig. 10(b) are due to the presence of hot and cold electron components. In the PIC/MC simulation [34] however two-temperature behavior of electrons are not observed clearly. In reverse, ion energy distribution in the sheath has two-temperature profile, which is consistent with the MC simulation result [11]. As it is not easy to measure the low-energy particle distribution experimentally, this simulation can produce the results that elucidate the experimental situation. The energy of ions in the tail portion is high and contributes to high sputtering rate. The energy distribution of ions impinging to the cathode is crucial in determining secondary emission of electrons as well as erosion rates.

The spatial electron and ion temperature distributions are shown in Fig. 11. Electron temperature has nearly the same value of a few electron volt throughout the plasma-bulk region except for the sheath region where it is 20–25 eV; these values agree with the measurements [3,42]. Near the cathode, the electron temperature is high and the starting point of temperature rising is associated with the sheath. Ion temperature profiles show quite different characteristics. Ion temperature along the *y*-direction does not vary much. But *x*- and *z*-direction temperatures are increasing towards the cathode. Especially in the *x*-direction (from the anode surface to cathode surface in Fig. 1) temperature rapidly increases towards the cathode. The results of MC simulation for ion energy at the cathode can be found in Ref. [11]. The temperature profile of the plasma is very important since incident ion temperature and direction are the quantities vitally related to surface reactions and ionization of background neutral gas. The high ion energy yields high sputtering rate, which is linearly dependent on the ion energy [43]. The erosion profile is also dependent on the ion energy because energetic ions have high sputtering rates.

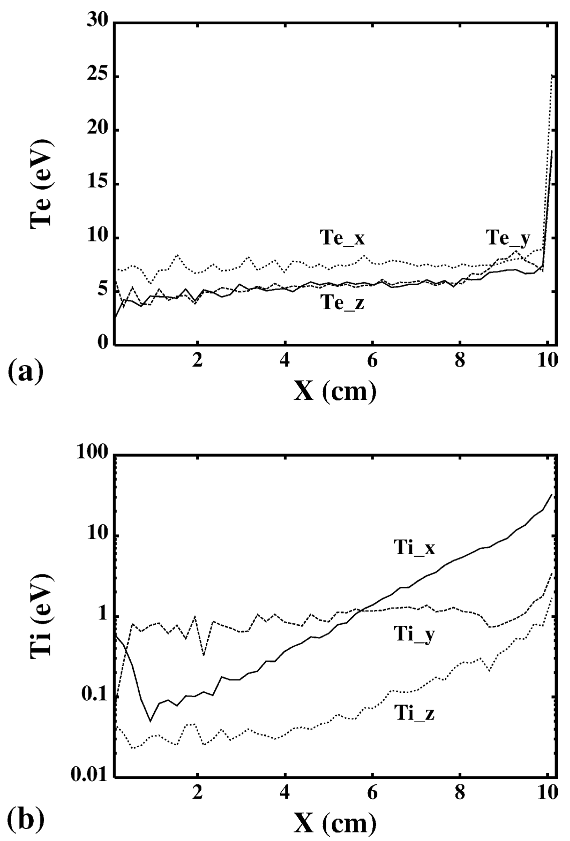

Fig. 11. Spatial temperature distributions of (a) electrons and (b) ions (from [34]).

5. Conclusions

Several topics concerning the simulation of magnetron sputtering systems are reviewed. There are many simulation results about magnetron sputter, which can be categorized as: (1) plasma simulation by MC method and PIC/MC method, (2) sputtered atoms simulation by MC method with or without neutral gas transport and (3) distribution functions and temperature profile calculation and comparison with experiment. Plasma simulation by MC method uses a prescribed potential profile and follows a fixed number of particles in order to obtain the collision information in the system. The collision (especially ionization) information is used for the estimation of the erosion profile. On the other hand, PIC/MC simulation calculates the potential profile self-consistently by the time evolution of charged particles. The ion flux towards target surface with energy distribution can be obtained easily from the simulation.

There are many simulations about the sputtered atoms transport. Sputtered atoms collide with background neutrals, transfer energy and momentum to the background neutral gas, and diffuse towards the substrate. The sputtered atom simulation usually includes the neutral gas simulation because the background neutral gas heating and rarefaction are closely related to the transport of sputtered atoms. The heating of background neutrals by sputtered atoms in front of the cathode is confirmed by comparison of MC simulation and experiment. The heating and rarefaction of neutrals in front of the cathode result in fewer collisions for sputtered atoms. The plasma profile is also affected by the change of background neutral gas distribution. Therefore the necessity increases for the unified simulation of plasma, sputtered atoms and background neutral gas as time goes on. As compared with the neutral gas and sputtered atoms, there are not many simulation results about the plasma distribution function calculation. As MC and PIC/MC simulation follow the velocities of particles, distribution function analyses will be followed in the future.

Acknowledgements

The financial supports from LG Electronics and the Ministry of Education of Korea through its BK21 program are gratefully acknowledged.

References

[1] J.A. Thornton, A.S. Penfold, Thin Film Processes, Academic Press, New York, 1974, p. 76.
[2] L. Gu, M.A. Lieberman, J. Vac. Sci. Technol. A 6 (1998) 2960.
[3] K. Kuwahara, H. Fujiyama, IEEE Trans. Plasma Sci. 22 (1994) 442;
K. Kuwahara, H. Fujiyama, Jpn. J. Appl. Phys. 36 (1997) 4922.
[4] A.E. Wendt, M.A. Lieberman, H. Meuth, J. Vac. Sci. Technol. A 6 (1998) 1827.
[5] A.E. Wendt, M.A. Lieberman, J. Vac. Sci. Technol. A 8 (1990) 902.
[6] Y.W. Choi, M. Bowden, K. Muraoka, Jpn. J. Appl. Phys. 35 (1996) 5858.
[7] H. Fujiyama, Y. Tokitu, Y. Uchikawa, K. Kuwahara, K. Miyake, K. Kuwahara, A. Doi, Surf. Coat. Technol. 98 (1998) 1467.
[8] K. Nanbu, S. Kondo, Vacuum 47 (1996) 1013;
K. Nanbu, S. Kondo, Jpn. J. Appl. Phys. 36 (1997) 4808.
[9] T.E. Sheridan, M.J. Goeckner, J. Goree, J. Vac. Sci. Technol. A 8 (1990) 30.
[10] T.E. Sheridan, M.J. Goeckner, J. Goree, J. Vac. Sci. Technol. A 8 (1990) 1623.
[11] M.J. Goeckner, J. Goree, T.E. Sheridan, IEEE Trans. Plasma Sci. 19 (1991) 301.
[12] W. Trennpohl Jr., J. Bretagne, G. Gousset, D. Pagnon, M. Touzeau, Plasma Sources Sci. Technol. 5 (1996) 607.
[13] J. Goree, T.E. Sheridan, Appl. Phys. Lett. 59 (1991) 1052.
[14] C.H. Shon, J.S. Park, B.K. Kang, J.K. Lee, Jpn. J. Appl. Phys., Part 1 38 (1999) 4440.
[15] E. Shidoji, K. Ness, T. Makabe, Vacuum 60 (2001) 299;
E. Shidoji, E. Ando, T. Makabe, Plasma Sources Sci. Technol. 8 (2001) 1;
E. Shidoji, H. Ohtake, N. Nakano, T. Makabe, Jpn. J. Appl. Phys., Part 1 38 (1999) 2131.
[16] R.D. White, R.E. Robson, K.F. Ness, J. Phys. D 34 (2001) 2205.
[17] V.V. Serikov, K. Nanbu, J. Vac. Sci. Technol. A 14 (1996) 3108.
[18] S. Ido, M. Kashiwagi, M. Takahashi, Jpn. J. Appl. Phys. 38 (1999) 4450.
[19] E. Shidoji, M. Nemoto, T. Nomura, Y. Yoshikawa, Jpn. J. Appl. Phys. 33 (1994) 4281.
[20] T. Kobayashi, K. Itagaki, T. Uchiyama, T. Tsukada, N. Hosokawa, Proceedings of the Third International Symposium on Sputtering and Plasma Processes, Tokyo, June 1995, p. 23.
[21] R.E. Somekh, J. Vac. Sci. Technol. A 2 (1984) 1285.
[22] T. Motohiro, J. Vac. Sci. Technol. A 4 (1986) 189.
[23] G.M. Turner, I.S. Falconer, B.W. James, D.R. Mckenzie, J. Vac. Sci. Technol. A 10 (1992) 455.
[24] H.M. Urbassek, D. Sibold, J. Vac. Sci. Technol. A 11 (1993) 676.
[25] Y. Yamamura, M. Ishida, J. Vac. Sci. Technol. A 13 (1995) 101.
[26] S.S. Nathan, G.M. Rao, S. Mohan, J. Appl. Phys. 84 (1998) 564.
[27] G.M. Turner, J. Vac. Sci. Technol. A 13 (1995) 2161.
[28] A. Bogaerts, R. Gijbels, V.V. Serikov, J. Appl. Phys. 87 (2000) 8334.
[29] V.V. Serikov, S. Kawamoto, K. Nanbu, IEEE Trans. Plasma Sci. 27 (1999) 1389.
[30] R. Kulka, Surf. Coat. Technol. 93 (1997) 1.
[31] N.F. Cramer, J. Phys. D 30 (1996) 2573.
[32] J.W. Bradley, G. Lister, Plasma Sources Sci. Technol. 6 (1997) 524.
[33] M.A. Lieberman, A.J. Lichtenberg, Principles of Plasma Discharges and Materials Processing, Wiley, New York, 1994.
[34] C.H. Shon, J.K. Lee, H.J. Lee, Y.K. Shin, Y. Yang, T.H. Chung, IEEE Trans. Plasma Sci. 26 (1998) 1635.
[35] T.E. Sheridan, J. Goree, J. Vac. Sci. Technol. A 7 (1989) 1014.
[36] S.M. Rossnagel, R.S. Robinson, J. Vac. Sci. Technol. A 1 (1983) 426.
[37] K. Okazawa, E. Shidoji, T. Makabe, J. Appl. Phys. 86 (1999) 2984.

[38] D.W. Hoffman, J. Vac. Sci. Technol. A 3 (1985) 561.
[39] S.M. Rossnagel, J. Vac. Sci. Technol. A 6 (1988) 19.
[40] T.E. Sheridan, M.J. Goeckner, J. Goree, J. Vac. Sci. Technol. A 9 (1991) 688;
T.E. Sheridan, M.J. Goeckner, J. Goree, J. Vac. Sci. Technol. A 16 (1998) 2173.
[41] F. Guimaraes, J. Bretagne, Plasma Sources Sci. Technol. 2 (1993) 127.
[42] S.M. Rossnagel, H.R. Kaufman, J. Vac. Sci. Technol. A 4 (1986) 1822.
[43] B. Chapman, Glow Discharge Processes, Wiley, New York, 1980.